

Utah State University

DigitalCommons@USU

Senior Theses and Projects

Materials Physics

12-2015

Predictive Formula for Electron Range over a Large Span of Energy

Anne C. Starley
Utah State University

JR Dennison
Utah State University

Follow this and additional works at: https://digitalcommons.usu.edu/mp_seniorthesesprojects

 Part of the [Condensed Matter Physics Commons](#)

Recommended Citation

Starley, Anne C. and Dennison, JR, "Predictive Formula for Electron Range over a Large Span of Energy" (2015). *Senior Theses and Projects*. Paper 22.

https://digitalcommons.usu.edu/mp_seniorthesesprojects/22

This Report is brought to you for free and open access by the Materials Physics at DigitalCommons@USU. It has been accepted for inclusion in Senior Theses and Projects by an authorized administrator of DigitalCommons@USU. For more information, please contact digitalcommons@usu.edu.



Predictive Formula for Electron Range over a Large Span of Energy

Revised 1/7/2016 14:20:00

Anne Starley

Mentor: JR Dennison

*Department of Physics, Utah State University,
4415 Old Main Hill, Logan, UT, USA 84322*

The research for this Physics 4900 final report was conducted by Anne Starley at Utah State University in the Spring and Fall semesters of 2015. Dr. JR Dennison served as the mentor for this research. Work was supported by an URCO grant awarded by the USU Office of Undergraduate Research and USU's Material Physics Group.

Keywords: Range, electron scattering, energy loss

I. ABSTRACT

A model developed by the Materials Research Group that calculates electron penetration range of some common materials, has been greatly expanded with the hope that such extensions will predict the range in other, perhaps, more interesting materials. Developments in this extended model aid in predicting the approximate penetration depth into diverse classes of materials for a broad range of energetic incident electrons (<10 eV to >10 MeV, with better than 20% accuracy). The penetration depth—or range—of a material describes the maximum distance electrons can travel through a material, before losing all of its incident kinetic energy. This model has started to predict a formula that estimates the penetration depth for materials without the need for supporting data, but rather using only basic material properties and a single fitting parameter (N_V , described as the effective number of valence electrons). N_V was first empirically calculated for 247 materials which have tabulated range and inelastic mean free path data in the NIST ESTAR and IMFP databases. Correlations of N_V with key material constants (*e.g.* atomic number, atomic weight, density, and band gap) were established for this set of materials. These correlations allow prediction of the range for additional materials which have no supporting data. These calculations are of great value for studies involving high electron bombardment, such as electron spectroscopy, spacecraft charging or electron beam therapy.

II. INTRODUCTION

The range, commonly known as the penetration depth, describes the maximum distance electrons can travel through a material, given an initial incident energy, before losing all of their kinetic energy and coming to rest.^{1,2} The primary energy loss mechanism which causes the electron to lose its kinetic energy is due to inelastic collisions within material.^{3,4}

In this experiment, the range functions as a single fitting parameter, N_V .

Due to the probabilistic nature of this mechanism, the Continuous Slow Down Approximation (CSDA) is often employed to simplify the problem where the stopping power is taken as a constant.

This idea is illustrated by a Lichtenburg discharged tree pictured in Fig. 1. This “tree” is an example of a situation where an accelerated high voltage electron comes to rest and deposits charge at a given range in an insulating material.⁵ The side view of the Lichtenburg tree displays the melted plastic caused by the energy of the deposited incident electrons at a uniform penetration depth. Here the stored charge is dissipated through a discharge.¹

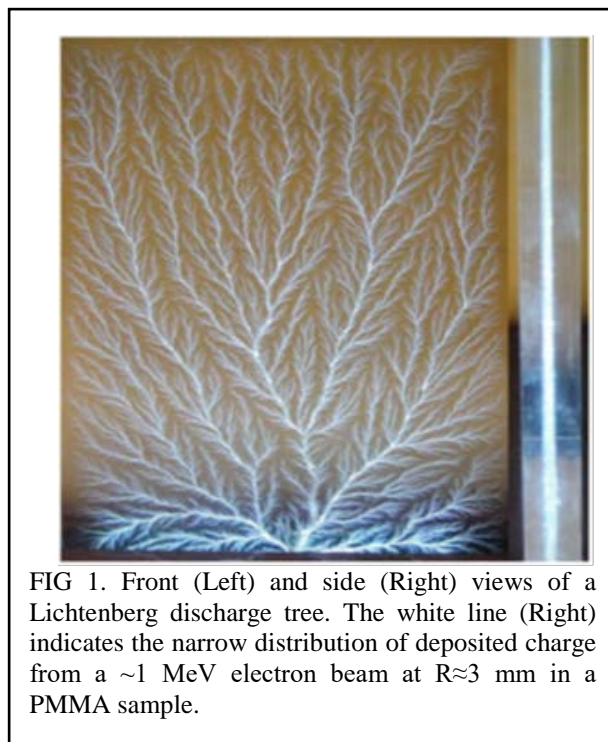


FIG 1. Front (Left) and side (Right) views of a Lichtenburg discharge tree. The white line (Right) indicates the narrow distribution of deposited charge from a ~ 1 MeV electron beam at $R \approx 3$ mm in a PMMA sample.

TABLE 1. Representative materials and specific material properties

| Materials | N_V | Density (gm/cm ³) | Mean Excitation Energy (eV) | Z^* (effective atomic number) | V_N (Effective atomic weight) |
|-------------|-------|-------------------------------|-----------------------------|---------------------------------|---------------------------------|
| Chromium | 3.0 | 0.093 | 0.838 | -0.431 | 0.828 |
| Gadolinium | 12.0 | 0.093 | 0.631 | -0.128 | 0.213 |
| PI (Kapton) | 3.6 | 0.036 | 0.666 | -0.315 | 0.452 |
| Oxide | 4.0 | -0.272 | 0.852 | -0.244 | 0.003 |
| Nickel | 7.0 | 0.045 | 0.966 | -0.641 | 0.438 |
| Radium | 15.0 | -0.067 | 0.693 | -0.166 | 0.576 |

III. ORIGINAL MODEL

The model previously developed by the Material Physics Group predicts the energy-dependent range, $R(E)$, as a function of incident electron energy for materials found in the NIST ESTAR database. In a continuous composite analytic approximation to the range with a single fitting parameter spanning incident energies, E , from <10 eV to >10 MeV, the following functions describe¹ the energy-dependent range, $R(E)$.

This first function is the range formula for low energy, medium energy, and high energy penetration;

$$R(E; N_V) = \begin{cases} \left[\frac{E}{E_m} \right] \frac{\lambda_{IMFP}(E_m)(1-\exp[-1])}{(1-\exp[-\frac{E}{E_m}])^2} & ; E < E_m \\ \left[\frac{E}{E_m} \right] \frac{\lambda_{IMFP}(E)}{1-\exp[-\frac{E}{E_m}]} & ; E_m \leq E \leq E_{HI} \\ bE^n \left(1 - \left[1 + \left[\frac{E/N_V}{m_e c^2} \right] \right]^{-2} \right) & ; E > E_{HI} \end{cases} \quad (1)$$

The second formula describes the mean energy lost per collision through the path that can further be described as a geometric mean of the band gap energy and Plasmon energy;

$$E_m = 2.8[E_{gap}^2 + E_p^2]^{\frac{1}{2}}. \quad (2)$$

The final function equates plasmon energy;

$$E_p = \hbar \left(\frac{N_V N_A \rho_m q_e^2}{m_e \epsilon_0 M_A} \right)^{\frac{1}{2}}. \quad (3)$$

Fits to these initial equations and optimum values of N_V were found using data from the material database. Figure 2 shows several approximate fits to the range data from the ESTAR database.²

IV. INITIAL PLAN

The first step to be taken on this project was the work of expanding the material database. An expanded list of materials and parameters could lead to equations that predict range of various known and unknown materials. Such information could be important in accurately and easily predicting the range of untested materials and would have great applications to fields such as spacecraft charging and radiation therapy.

After the initial work of correcting, collecting, and expanding the material database, studying fits based on the extended parameters was next. However, it was discovered that one of the more important parameters - the material band gap -- was often difficult to find. Special attention was given to band gap, and extended searches through the literature were necessary. It also became essential to find the affordable margin of error for this parameter before we could proceed.

While looking at our single parameter N_V as a function of density, mean atomic weight, mean atomic number, plasmon energy or bandgap, conductivity, phase, and more we planned to fit the information. Such correlations would tell us how to proceed in finding new functions that cover a wide range of fits very well using a theoretical equation. These findings could lead to accurate predictions of the range of more complex materials and biological materials like bone, soft tissue, and cartilage that could be used in radiotherapy applications.

We once again hit a small snag when we realized that our fits would not be able to be predicted linearly and a more advanced method would be needed to accurately find a range formula. More information can be found in the following subdivisions.

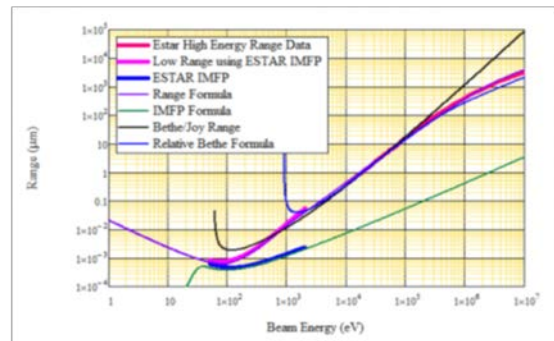


FIG 2. Comparison between several range approximations and the data from the ESTAR database for Au. The IMFP data for Au are also plotted along with the TPP-2M IMFP formula for $\lambda_{IMFP}(E)$.

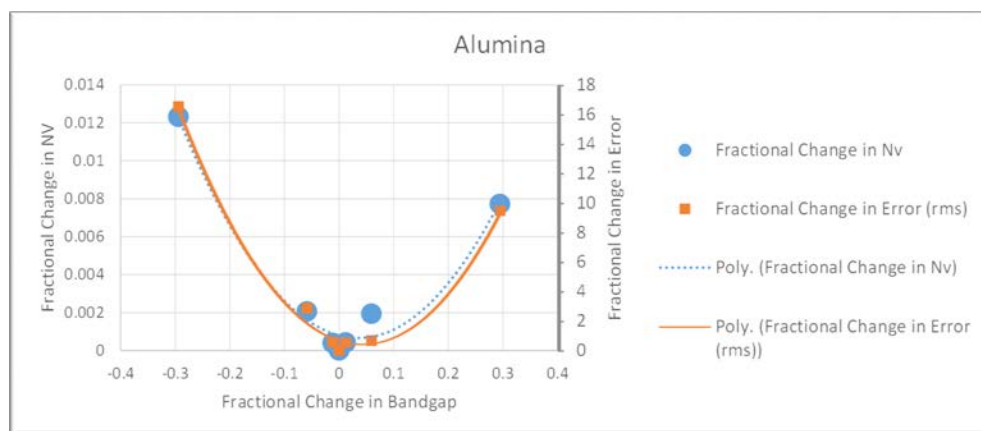


FIG 3. The fractional change in the band gap versus the fractional change in N_V and the fractional change in error.

V. EXPANDING DATABASE

The first steps in expanding the range model involved expanding the material database in both number of materials and parameters used. To further validate the range formulations and to lead to possible new discoveries in range penetration, the Material Physics Group's material database needed to be enlarged and corrected.

A spreadsheet had previously been compiled with information on a number of materials. The spreadsheet's minor errors were revised and both the total number of materials in the database and parameters for each material were extended. (e.g., considerations such as phase, color, and conductivity were added).

The greater number of materials allowed for a more exact fit to be determined with the CSDA. Adding more parameters offered the opportunity of exploring possible trends that might enable a discovery of an even more exact function to describe the range.

Table 1 offers a small selection of the compiled materials, along with some of the materials' applicable physical properties and shows some of the results of the material database expansion.

VI. AFFORDABLE MARGIN OF ERROR

In order to perform range calculations, a value for the electron band gap was needed for each material. However, band gap proved a tricky parameter to find. This was our

next step in discovering a good predictive range model. While some material band gaps were easier to ascertain than others, it was necessary for a comparison to be made to see how much the fitting factor would change with a varying bandgap value.

These calculations gave desirable results, showing that the fitting factor varied minimally with changing bandgaps. For an example, see Figure 3,

which uses alumina (Al_2O_3) as the chosen material.

Further results showed that the error between the values in our calculations and the values in the NIST database increased as the band gap's value increased from the true value.

In order to put the fitting factor variances into perspective, Fig. 4 shows what alumina's fit for the range approximation would look like if we had used an N_V of 0.10, 4.05 (the calculated value), and 8.00. Based on these results, even with significant variance in N_V we can expect to find values that are reasonably accurate for most applications.

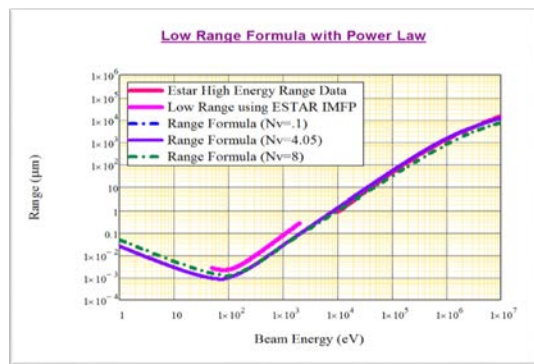


FIG. 4. Three different N_V are applied to alumina (0.10, 4.05, and 8.00), and the fits compared.

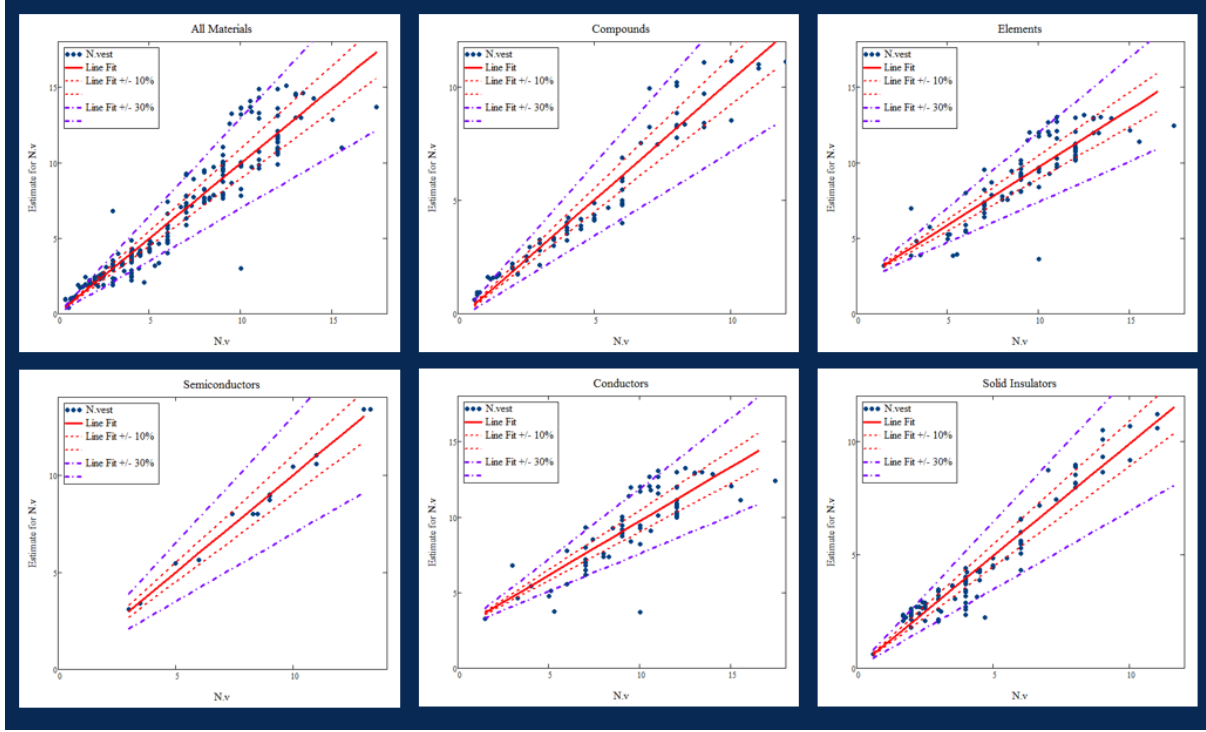


FIG 5. Examining different subsets of materials to help determine what effects these subsets might have.

VII. FORMULATION FOR ANALYTIC SOLUTION

The next step taken in developing our range formula was creating an analytical solution based on a theoretical formula. The following theoretically formula for the effective number of valence electrons (or the range),

$$N_V = A\rho^B M_A^C Z^D \quad (4)$$

where A is a constant, ρ is density, M_A is the effective atomic weight, Z is the effective atomic number, and B , C , and D are possible powers these parameters might be raised to, was utilized as a model of our own future fit.

This predictive formula was used in order to look at our single parameter N_V as a function of various factors. The information gathered in the analysis was fit to N_V in hopes of finding strong trends between variables like density, effective atomic weight, mean atomic number, plasmon energy or bandgap, conductivity, phase, and more.

Continual modification to the range model using our theoretical equation (Eq. 4) could lead us to universal values for A , B , C , and D .

Equations were further subcategorized into groupings such as insulators, conductors, and semiconductors and solids, liquids, and gasses with the hope that different trends with different parameters would be discovered. Perhaps equations for conductors versus insulators and

semiconductors would have somewhat different values for A , B , C and D .

An analytical solution was created to greatly increase the ease with which the fitting parameters in the theoretical formula could be found. First a power law regression for N_V was modeled using the method of Best Estimates. To minimize χ^2 the partial derivative with respect to each fitting parameter was calculated and set to zero. This gave a series of linear equations which were put into a matrix form giving a standard eigenvalue problem. The fitting parameters was then used to calculate an estimate of N_V using the power law model.⁷

Plotting this estimate of N_V versus the true value of N_V allowed us to quantify the quality of the fit as can be seen in Figure 5.

Figure 5 examines different subsets of materials to help determine what effects these subsets might have on the fitting parameters. In this figure, the variables A , B , C , and D are the powers to which density, mean atomic weight, mean atomic number, and effective atomic number are raised to respectively.

In order to find the best fit, a linear fit of N_V and the estimate N_V were found with a reported χ^2 . Nominally the slope of the fit would be 1 with an intercept of zero. Thus, looking at only χ^2 does not give us enough information to determine if the fit was acceptable or not. 10% and 30% error lines to the slope are marked in dashed red and dashed purple lines, respectively.

TABLE 2. Fitting Parameters for the graphs in Fig. 6 as well as the linear fit statistics.

| Materials | A | B | C | D | χ^2 | Slope | Intercept |
|------------------|-------|--------|-------|--------|----------|-------|-----------|
| All | 0.811 | 0.093 | 0.838 | -0.431 | 0.828 | 0.994 | 0.022 |
| Compounds | 0.749 | 0.093 | 0.631 | -0.128 | 0.213 | 1.052 | -0.230 |
| Elements | 1.268 | 0.036 | 0.666 | -0.315 | 0.452 | 0.767 | 2.034 |
| Semiconductors | 0.764 | -0.272 | 0.852 | -0.244 | 0.003 | 1.002 | -0.017 |
| Conductors | 1.047 | 0.045 | 0.966 | -0.641 | 0.438 | 0.717 | 2.574 |
| Solid Insulators | 0.842 | -0.067 | 0.693 | -0.166 | 0.576 | 0.989 | 0.014 |

Values for the fitting parameters and the linear fit statistics can be found in Table 2.

Development of this analytic formula and graphing process greatly simplified the process of looking for theoretical values of various subsets and will ease future work on this project.

VIII. APPLICATIONS

The range model developed predicts the penetration depth for various materials for different incident electrons. It's effects extend to spacecraft charging where the range is used to predict the distribution of incident electrons produced by the space plasma environment within materials as well as the energy deposited by the electrons as they travers through materials. This information can further be used to predict and describe the resulting conductivity and discharging in solids.¹

The range is also used in Electron Beam Therapy, (pictured in Fig. 6) the most common form of medical radiotherapy. Range calculations can be used to inform technicians operating Electron Linear Accelerators of the depth and distribution of the externally applied radiation and aid in determining the applied dose.⁶ Obtaining accurate, reliable, and efficient information on the range of electron penetration is, therefore, extremely important to the medical community.



FIG 6. Medical radio therapy.

IX. FUTURE DIRECTION

We plan to continue the work on the project by searching for more trends in our data as we manipulate the analytical solution. We hope that these trends will give us clues into how to further assemble and perfect our range formulas.

After these functions have been found, we plan to create a website that will share our finding with the scientific community. This website will also be able to estimate the range of an unknown material to a percent accuracy when a user enters necessary known information. This website can be utilized by any of the aforementioned fields that deal directly with electron range penetration.

1. ACKNOWLEDGEMENTS

I gratefully acknowledge the financial support given by an URCO grant awarded by the USU Office of Undergraduate Research, as well as the extensive help received from USU's Material Physics Group, especially by members Lisa Phillipps, Greg Wilson, and JR Dennison.

1. Wilson, G., & Dennison, J.R. (2010). Approximation of range in materials as a function of incident electron energy.
2. Teancum Quist (with Greg Wilson and JR Dennison), "Compilation and Comparison of Electron Penetration Ranges as a Function of Effective Number of Valence Electrons," Utah State University, Logan, UT, April 2013.
3. S. Tanuma, C. J. Powell and D. R. Penn, 2004, "Calculations of electron inelastic mean free paths. V. Data for 14 organic compound over the 50-200 eV range," Surface and Interface analysis 21, 3. pp 165-176.
4. H. J. Fitting, H. Glaefcke and W. Wild, 2006, "Electron penetration and energy transfer in solid targets," Physica statut solidi 41, 1.

5. Starley, A., Philipps, L., Dennison, J.R., "Electron Range Penetration for Various Materials" U.R.C.O Proposal, Utah State University, Logan, UT, 2015
6. . J. Sempau, S.J. Wilderman, and A.F. Bielajew, 2000, "DPM, a fast, accurate Monte Carlo code optimized for photon and electron radiotherapy treatment planning dose calculations," *Physics in Medicine and Biology* 45, 8.
7. Taylor, John R. (1997). *An Introduction to Error Analysis: The Study of Uncertainties in Physical Measurements. Second Edition*. University Science Books. Sausalito, CA.